Supramolecular Self-assemblies of Inverted Cucurbit[6]uril with 1,5-pentanediamine

Zhi-Nian Liu,[a] Jian-Hang Hu,[a] Yu Xiong,[a] Jia-Yi Zhang,[a] Run-Xin Hou,[a] Chun-Rong Li,[b]* Tie-Hong Meng,[b] Timothy J. Prior,[c] Carl Redshaw,[c] Xin Xiao*[a]

[a] Key Laboratory of Macrocyclic and Supramolecular Chemistry of Guizhou Province, Guizhou University, Guiyang 550025, China.

[b] Public Course Teaching Department, Qiannan Medical College for Nationalities, Duyun, 558000, China

[c] Chemistry, School of Natural Sciences, University of Hull, Hull HU6 7RX, U.K.

E-mail: gyhxxiaoxin@163.com, xxiao@gzu.edu.cn (Xin Xiao); lichunrong68@163.com (Chun-Rong Li).

Abstract: In this study, single crystal X-ray diffraction and ^{1}H NMR spectroscopy were used to examine the interaction of the guest 1,5-pentanediamine with inverted cucurbit[6]uril (*i*Q[6]) in the presence of $[ZnCl_4]^{2-}$ anion. The results show that $[ZnCl_4]^{2-}$ and $[Zn(H_2O)Cl_3]^-$ anions form a honeycomb framework structure, and *i*Q[6] forms a 1:1 complex with 1,5-pentanediamine. Inverted cucurbit[6]uril forms molecular chains via outer surface interactions, which in turn fill in the honeycomb framework structure. The amino groups at both ends of the 1,5-pentanediamine guest are situated at the entrance of the central cavity, while the alkyl chain part resides in the central cavity of the *i*Q[6].

Keywords: Inverted cucurbit[6]uril; 1,5-pentanediamine; supramolecular assembly; tetrachlorozincate anion; honeycomb framework.

1. Introduction

Biogenic amines (BAs) are nitrogenous organic compounds important to living organisms [1] and can be classified according to their chemical structure as aliphatic amines (cadaverine, spermidine, putrescine), aromatic amines (dopamine, phenylethylamine, tyramine) or heterocyclic amines (tryptamine, histamine) [1-6]. Cadaverine, also known as 1,5-pentanediamine, is produced when a corpse is broken down by bacteria. Cadaverine is a fatty amine of the biogenic amine family and has a variety of biological functions. It is a common constituent of high-protein foods including fish, pork, soy, as well as different beverages and wines, and particularly dairy products [7-9].When manufacturing and storage conditions are favorable for microbial development, microbial contamination can result in lysine decarboxylation, aldo-ketoamidation and transamidation, which can produce cadaverine [1, 10, 11]. Therefore, 1,5-pentanediamine can be used as a decomposition marker and a key indicator of the quality and freshness of high-protein industrial foods such as meat [12-14]. Like other biogenic amines, cadaverine exhibits a range of physiological and toxicological effects depending on concentration. Cadaverine is an essential component of many physiological processes in living things, acting not only as a source of nitrogen but also as a blood pressure control, and impacts on pH and cell metabolism and growth at low concentrations [15-17]. At high concentrations, cadaverine enhances the toxicity of histamine and can combine with nitrite to form the cancer and mutagenic substance nitrosamines. Cadaverine can also have several negative side effects, including headaches, nausea, vomiting, diarrhea, hypotension, and bradycardia [15, 18-21]. A significant industrial chemical with numerous uses, cadaverine can be used as a raw material in the production of polyamides and polyurethanes [22-24]. As a result, it is crucial to identify 1,5-pentanediamine and analyze its behavior in quantitative fashion if possible. To-date, researchers have reported a number of techniques for the separation and analysis of biogenic amines, including immunoassays, capillary electrophoresis, enzymatic methods, and fluorescence-high performance liquid chromatography [25-28].

In macrocyclic compounds, guest molecules can be incorporated and can interact in non-covalent fashion with their hosts, forming supramolecular systems that are the perfect

platform for molecular recognition. Such a strategy has attracted extensive attention in recent years, and the recognition of biogenic amine molecules by various supramolecular host compounds (crown ethers, cyclodextrins, calix[*n*]arenes and pillar[*n*]arenes) has been reported [29-32].

Cucurbit[*n*]urils (Q[*n*]s), originally obtained as a white solid compound by the reaction of glycourea unit with formaldehyde under acidic conditions by the German chemist Behrend [33], are a class of macrocyclic hosts compounds different from crown ethers, cyclodextrins, calix[*n*]arenes and pillar[*n*]arenes. The prominent feature of Q[*n*]s is a rigid hydrophobic cavity that varies in size and affinity with the degree of polymerization and is lined with upper and lower ports of hydrophilic carbonyl oxygen atoms [4, 34-36], which allows guest molecules to enter through two open ports, thus wrapping them in the empty cavity of the Q[*n*]s. In addition, the guest molecule can interact with the outer surface of the Q[*n*]s through weak noncovalent interactions (hydrogen bonding, π-π stacking, C-H···π and ion-dipole interactions), known as the "outer-surface interaction" of cucurbit[*n*]urils [37-39]. It is due to the aforementioned properties that the Q[*n*] family has received extensive attention. The use of Q[*n*]-based supramolecular assemblies in chemical catalysis, drug delivery, sensors, biomolecular recognition, etc. has been reported by various researchers[40-47]. In 2005, Isaacs and Kim reported both the inverted cucurbit[6]uril (*i*Q[6]) and inverted cucurbit[7]uril (*i*Q[7]) [48]. The inverted cucurbit[*n*]uril family has an inverted glycourea unit, which makes the cavity of the inverted cucurbit[*n*]uril different from that of the normal cucurbit[*n*]uril[49, 50], and given the difficulty in isolating such inverted species from the cucurbit[*n*]uril mixture, these inverted cucurbit[*n*]urils have rarely been reported. However, the different structural features possessed by inverted cucurbit[*n*]urils *versus* normal cucurbit[*n*]urils, and given that their encapsulation behavior of guest molecules may also differ from that of the normal cucurbit[*n*]urils, such inverted species deserve further in-depth exploration [51-53].

In the present work, we have explored how the macrocyclic host *i*Q[6] forms supramolecular assemblies with biogenic amine molecules in the presence of structure inducers. In this study, a 1:1 supramolecular assembly of 1,5-pentanediamine and *i*Q[6]

was constructed in 6 M HCl medium using *i*Q[6] as the host component and $[ZnCl_4]^{2-}$ as the structure inducer. The complexation behavior of the host *i*Q[6] and the guest 1,5-pentanediamine in solution was investigated using ^{1}H NMR spectroscopy and X-ray crystallography. Figure 1 shows the structures of the inverted cucurbit[6]uril (*i*Q[6]) and 1,5-pentanediamine.

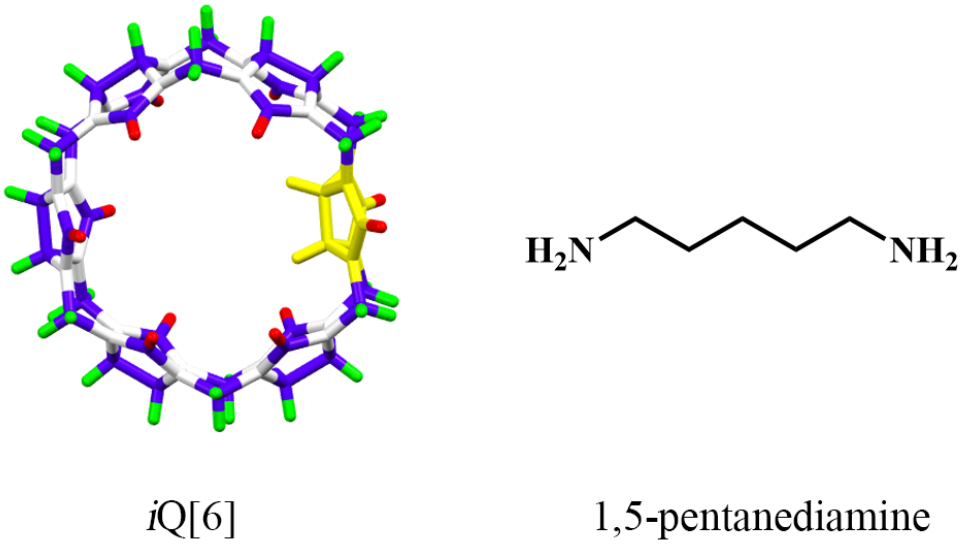

*i*Q[6] 1,5-pentanediamine

Figure 1. Chemical structures of *i*Q[6] and the guest 1,5-pentanediamine.

2.Experimental section

2.1 *Materials*

The guest 1,5-pentanediamine was purchased from Aladdin and was used without further purification; it was protonated in the presence of 6 M HCl. *i*Q[6] was prepared and purified according to the literature methods [45, 47, 48]. Deionized water was used during all the experiments.

2.2 *^{1}H NMR spectroscopy*

The complexation reaction of *i*Q[6] with 1,5-pentanediamine in solution was studied by ^{1}H NMR spectroscopy at 298.15 K, using 4 M DCl/D_2O, and were recorded on a JEOL JNM-ECZ400S 400 MHz NMR spectrometer (JEOL). D_2O was used as a field frequency lock, and the observed chemical shifts were reported in parts per million (ppm) relative to the internal standard (TMS of 0.0 ppm).

2.3 *Single-crystal X-ray crystallography*

Colorless single crystals suitable for X-ray diffraction were obtained by slow evaporation of a 6 M HCl solution over about one week. A suitable crystal (about 0.2 × 0.2 × 0.1 mm^3) were taken, fixed on a glass filament with petroleum jelly, and diffraction data were collected on a Bruker Smart Apex III X-ray single crystal diffractometer. A Mo target with an excitation voltage of 50 KV for Mo, and a wavelength λ(MoKα) = 0.71073 Å were used at a temperature of 293 K. Empirical absorption corrections were applied by using the multi-scan program SADABS. The data were reduced and corrected using Lp correction with both polarized factor correction and Lorentz factor correction, and semi-empirical absorption correction. Structure solution was conducted by direct methods using the SHELXS-97 program and full matrix least squares refinement of F^2 values by the SHELXL-2018 program for the anisotropic refinement of all non-hydrogen atoms with Olex2. Carbon-bound hydrogen atoms were introduced at the calculated positions and treated as riding atoms with isotropic displacement parameters of 1.2 times the displacement parameter of the parent atom. Disordered solvent was modelled using a solvent mask. CCDC 2259121 contains the complex *i*Q[6]@1,5-pentanediamine with additional crystallographic data.

2.4 *Preparation of complex A*

*i*Q[6] (20 mg, 0.02 mmol) and $ZnCl_2$ (13.9 mg, 0.12 mmol) were weighed out and dissolved in 6 M HCl (1.0 mL), heated and stirred until completely dissolved, and cooled to obtain solution V1. 1,5-Pentanediamine (14.3 mg, 0.14 mmol) was then placed in a vial and dissolved by adding 1.0 mL H_2O to obtain solution V2; the latter was then added to solution V1 and mixed well with stirring. After standing for about 10 days, crystals were obtained (compound A), $(C_5H_{16}N_2)$@*i*Q[6]·$[ZnCl_4]$·$[Zn(H_2O)Cl_3]$·(H_3O)·2(H_2O). The data and structural refinement details of compound A are given in Table 1.

Table 1：Compound A single crystal data and refined structure.

Empirical formula	$C_{41}H_{61}Cl_7N_{26}O_{16}Zn_2$
Formula weight	1553.24
Crystal system	monoclinic
Space group	$P2_1/n$
a, Å	14.8476(13)
b, Å	22.5459(19)
c, Å	22.2940(19)
α, deg	90.00
β, deg	91.380(3)
γ, deg	90.00
V, $Å^3$	7460.8(11)
Z	4
Dcalcd, g cm^{-3}	1.383
T, K	293(2)
μ, mm^{-1}	0.965
Unique reflns	13293
Obsd reflns	8383
Params	791
Rint	0.0591
R [I>2σ (I)]	0.0503
wR(F^2) [I>2σ (I)]	0.1351
R(all data)	0.0768
wR(F^2) (all data)	0.1454
Goof on F^2	1.026

3. Results and discussion

3.1 *Analysis of crystal structure*

It is well known that $[CdCl_4]^{2-}$ and $[ZnCl_4]^{2-}$ anions can play the role of structural directing agents in the construction of Q[*n*]-metal coordination polymers. In the present work, the introduction of $[ZnCl_4]^{2-}$ into the *i*Q[6]-1,5-pentanediamine system demonstrated the formation of supramolecular assemblies of 1,5-pentanediamine with *i*Q[6] molecules in the presence of $[ZnCl_4]^{2-}$ anions.

Single-crystal X-ray diffraction data revealed the formation of a supramolecular self-assembly system of compound A (*i*Q[6]-1,5-pentanediamine-$[ZnCl_4]^{2-}$-HCl). This structure was formed by the interaction of Zn^{2+} in 6 M hydrochloric acid medium forming $[ZnCl_4]^{2-}$ ions and $[Zn(H_2O)Cl_3]^-$ ions, and $[ZnCl_4]^{2-}$ was introduced into the system of *i*Q[6]-1,5-pentanediamine-HCl. The *i*Q[6] and the zinc complexes were clearly identified in the structure and were well resolved from the diffraction data. The 1,5-pentanediamine was much more poorly located; there is a clear region of electron density located within the *i*Q[6] consistent with a linear molecule but this electron density is rather diffuse. The encapsulated molecule was modelled as disordered over 2 different positions. This is physically meaningful and provides a reasonably good fit to the data, but is still probably a much more ordered arrangement than is actually present in the crystal.

First, we focus on the part of the crystal structure, as shown in Figure 2a, where a hexagonal honeycomb framework structure is formed in compound A by $[ZnCl_4]^{2-}$ and $[Zn(H_2O)Cl_3]^-$ ions. The *i*Q[6] molecules form one-dimensional supramolecular chains through outer-surface interactions before filling into the honeycomb cavity. As shown in Figure 2b, a closer look reveals that each *i*Q[6] molecule is surrounded by three $[ZnCl_4]^{2-}$ and four $[Zn(H_2O)Cl_3]^-$ ions, which are driven by the $[ZnCl_4]^{2-}$ anion interacting with the $[Zn(H_2O)Cl_3]^-$ anion and the positively charged outer wall of *i*Q[6] through the outer wall of the cucurbit[*n*]uril. The water molecule of the $[Zn(H_2O)Cl_3]^-$ anion forms a hydrogen bond to one portal carbonyl oxygen of *i*Q[6] with O…O distance of 2.812 Å. In addition, the chloride ions of $[ZnCl_4]^{2-}$ and $[Zn(H_2O)Cl_3]^-$ form

a large number of C-H…Cl interactions with the hydrogen on the bridging methylene and the glyoxal unit on the waist of *i*Q[6], where the $[ZnCl_4]^{2-}$ forms interactions with bond distances between 2.632 Å and 2.941 Å, and $[Zn(H_2O)Cl_3]^-$ forms interactions with bond distances between 2.712 Å and 2.913 Å. One of the chloride ions of $[Zn(H_2O)Cl_3]^-$ forms an interaction with the carbon on the *i*Q[6] bridging methylene with a distance of 3.449 Å for Cl(6)-C(19). In Figure 2c, we omitted the anion from the structure for ease of observation and kept only the cucurbit[*n*]uril and the guest molecule. Although the guest is poorly resolved, there is evidence that the protonated amine (as NH^{3+}) forms charge-assisted hydrogen bonds to the portal oxygen atoms. O(1)⋯H(25B) 2.585 Å, O(2)⋯H(25B) 2.347 Å, O(2)⋯H(25C) 2.512 Å, O(3)⋯H(25C) 2.501 Å, O(9)⋯H(26B) 2.412Å, and C-H⋯O interactions may play a role in helping to locate the diamine in the cavity.

Closer inspection of the cucurbit[*n*]uril self-induced outer wall interactions reveals that each *i*Q[6] molecule is surrounded by four adjacent *i*Q[6] molecules. The *i*Q[6] molecule is connected by the formation of interactions between the port carbonyl oxygen atom and the carbonyl carbon of the adjacent *i*Q[6] molecule, where two C(3)⋯O(34) interactions have a bond distance of 3.191 Å and the other two C(1)⋯O(10) interactions have a distance of 3.156 Å (Figure 2d).

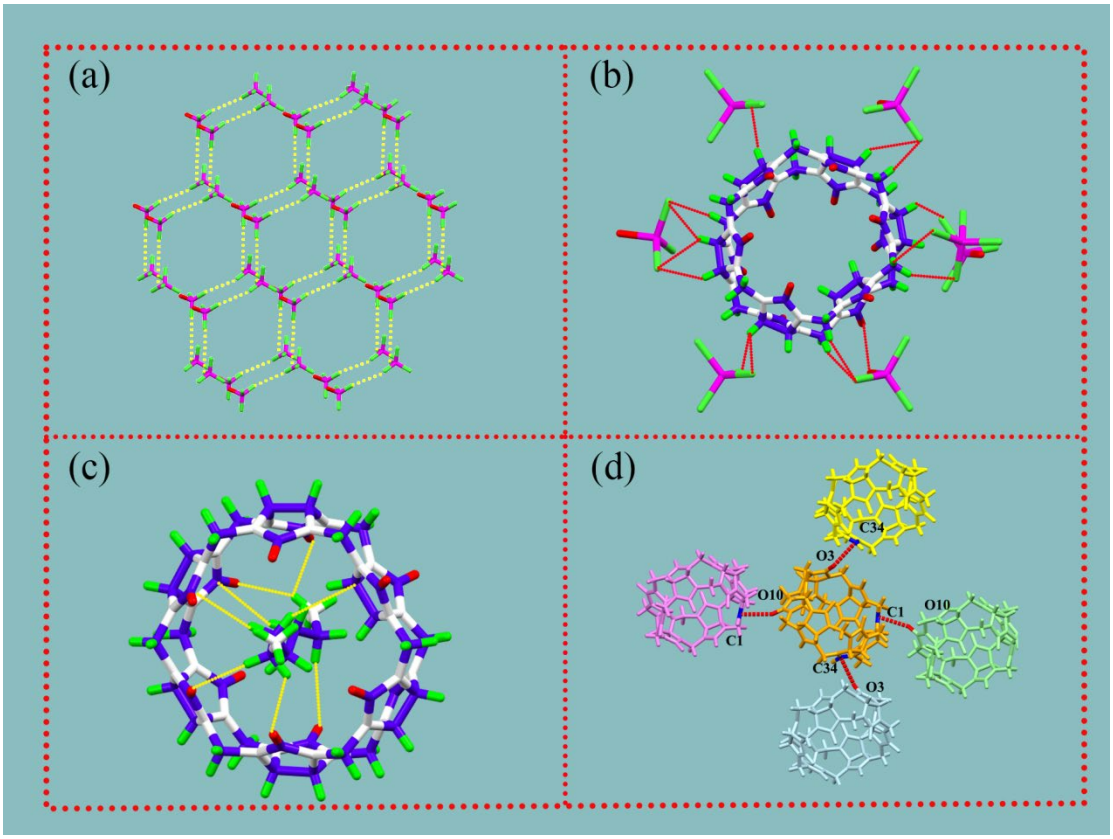

Figure 2. (a) Honeycomb framework structure formed by $[ZnCl_4]^{2-}$ ions and $[Zn(H_2O)Cl_3]^-$ ions; (b) interactions between $[ZnCl_4]^{2-}$ and $[Zn(H_2O)Cl_3]^-$ and *i*Q[6]; (c) interactions between *i*Q[6] and the guest 1,5-pentanediamine; (d) each *i*Q[6] (red) is surrounded by four *i*Q[6] molecules through outer surface interactions.

As shown in Figure 3a, the *i*Q[6] molecule has a positively charged outer surface and forms a one-dimensional linear assembly through its own outer surface interactions. Two adjacent *i*Q[6] molecules are connected by C···O interactions, the carbonyl oxygen (O3) of one *i*Q[6] molecule is attached to the carbon atom (C34) of another *i*Q[6] molecule at a separation of around 3.191 Å for C(34)···O(3). Furthermore, the two-dimensional planar structure constructed based on the one-dimensional supramolecular chain is shown in Figure 3b, exhibiting a parallelogram porous channel with a cross-sectional area of 55.1 $Å^2$ along the *a*-axis direction formed by the *i*Q[6] molecule and the 1,5-pentanediamine guest molecule. In Figure 3c, based on the above two-dimensional structure, the three-dimensional spatial pore channel of each

quadrilateral is formed by eight *i*Q[6] molecules helically wound around the axis. It can be seen that the *i*Q[6] molecules are connected to the $[ZnCl_4]^{2-}$ and $[Zn(H_2O)Cl_3]^-$ anions through ion-dipole interactions and to the other *i*Q[6] molecules through outer surface interactions.

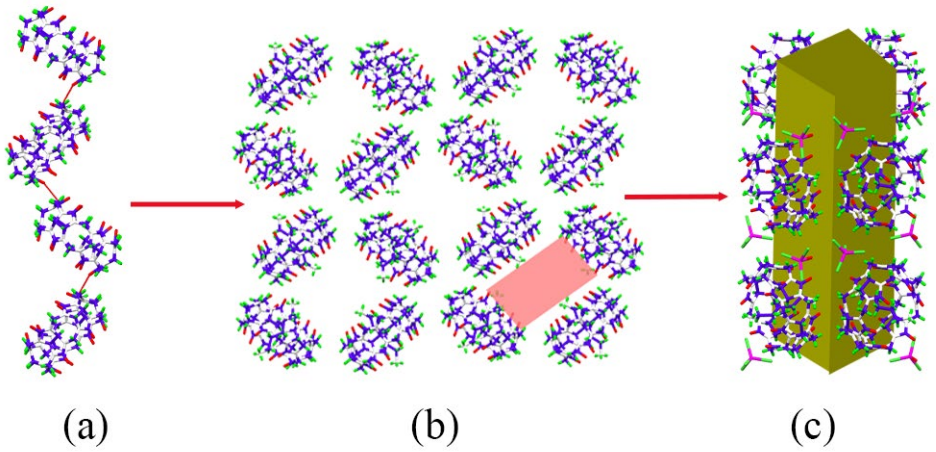

Figure 3. (a) Ion-dipole interactions between two adjacent *i*Q[6] molecules; (b) general top view of the supramolecular assembly consisting of *i*Q[6] and the guest 1,5-pentanediamine along the *a*-axis; (c) pore structure consisting of *i*Q[6]-1,5-pentanediamine-$[ZnCl_4]^{2-}$.

After examining the individual parts, our interest turns to the structure of the entire supramolecular complex assembly. As shown in Figure 4a, two adjacent *i*Q[6] molecules form a one-dimensional supramolecular chain-like structure by forming weak interactions with $[ZnCl_4]^{2-}$ ions and $[Zn(H_2O)Cl_3]^-$ ions, where the methyl or methylene group on the outer surface of the *i*Q[6] molecule interacts with the neighboring *i*Q[6] molecules by an outer-surface interaction (O10···C1). In addition to the ion-dipole interaction of two adjacent *i*Q[6] molecules with a $[ZnCl_4]^{2-}$ ion and a $[Zn(H_2O)Cl_3]^-$ ion as in Figure 4b, the $[ZnCl_4]^{2-}$ and $Zn(H_2O)Cl_3]^-$ are connected to the methyl or methylene hydrogen on the outer wall of the *i*Q[6] molecule by ion-dipole interactions. The $[ZnCl_4]^{2-}$ forms three C-H···Cl^- interactions with *i*Q[6], the distance of C-H···Cl^- is between 2.632 Å and 2.941 Å, whilst $[Zn(H_2O)Cl_3]^-$ forms six C-H···Cl^- interactions and one hydrogen bond with *i*Q[6], the distance of C-H···Cl^- is between

2.721 Å and 2.913 Å, and the O-H···O distance is 2.044Å. The supramolecular component as shown in the crystal stacking diagram formed by the interaction of the *i*Q[6] molecule, the guest 1,5-pentylenediamine, $[ZnCl_4]^{2-}$ and $Zn(H_2O)Cl_3]^-$, as shown in Figure 4c, contrasts with the results found for the interaction with other guests such as 1,*ω*-alkylenediamines, for example *i*Q[6] forming a ternary V-shaped supramolecular chain with ethylenediamine, and with hexanediamine which produces a pseudorotaxane conformation [45,46].

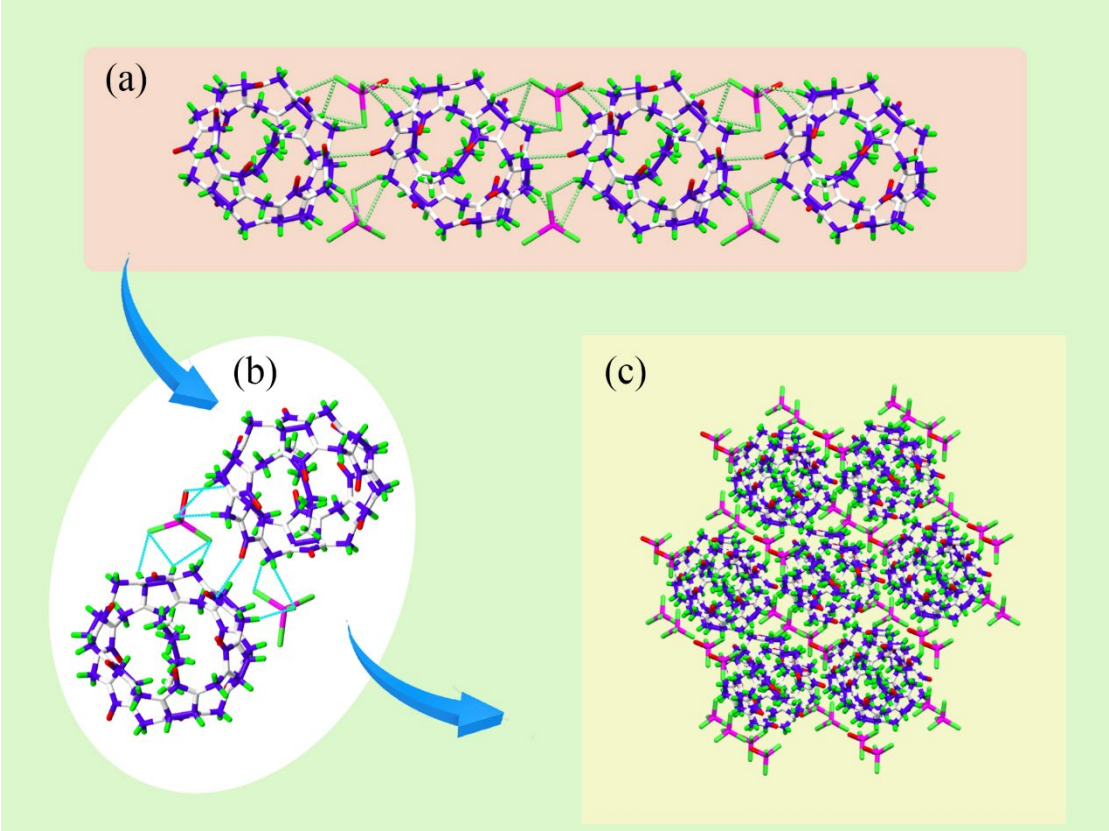

Figure 4. (a) Molecular chain formed by *i*Q[6] molecule, guest 1,5-pentanediamine, $[ZnCl_4]^{2-}$ and $[Zn(H_2O)Cl_3]^-$; (b) two adjacent *i*Q[6] molecules with $[ZnCl_4]^{2-}$ and $[Zn(H_2O)Cl_3]^-$ interactions; (c) top view of supramolecular assemblies formed by *i*Q[6] molecules, guest 1,5-pentanediamine, $[Zn(H_2O)Cl_3]^-$ and $[ZnCl_4]^{2-}$.

3.2 *^{1}H NMR spectroscopy*

The host-guest interaction pattern of *i*Q[6] with the 1,5-pentanediamine guest can be detected by ^{1}H NMR spectroscopic experiments, whereby 1,5-pentanediamine was

added to the *i*Q[6] solution. The hydrophobic cavities of the Q[*n*]s are proton shielding regions, so they cause an up-field shift of the corresponding proton signals. As shown in Figure 5, the ^{1}H NMR spectrum of the guest 1,5-pentanediamine changed significantly with upfield shifts of the methylene protons H(α), H(β) and H(γ), with H(α) shifted from 1.75 ppm to 1.72 ppm, H(β) shifted from 0.44 ppm to 0.39 ppm and H(γ) shifted from 0.18 ppm to 0.13 ppm, which indicates that the alkyl chain part of the 1,5-pentanediamine is completely wrapped in the hydrophobic cavity of the *i*Q[6]. These observations are consistent with the X-ray diffraction analysis described above.

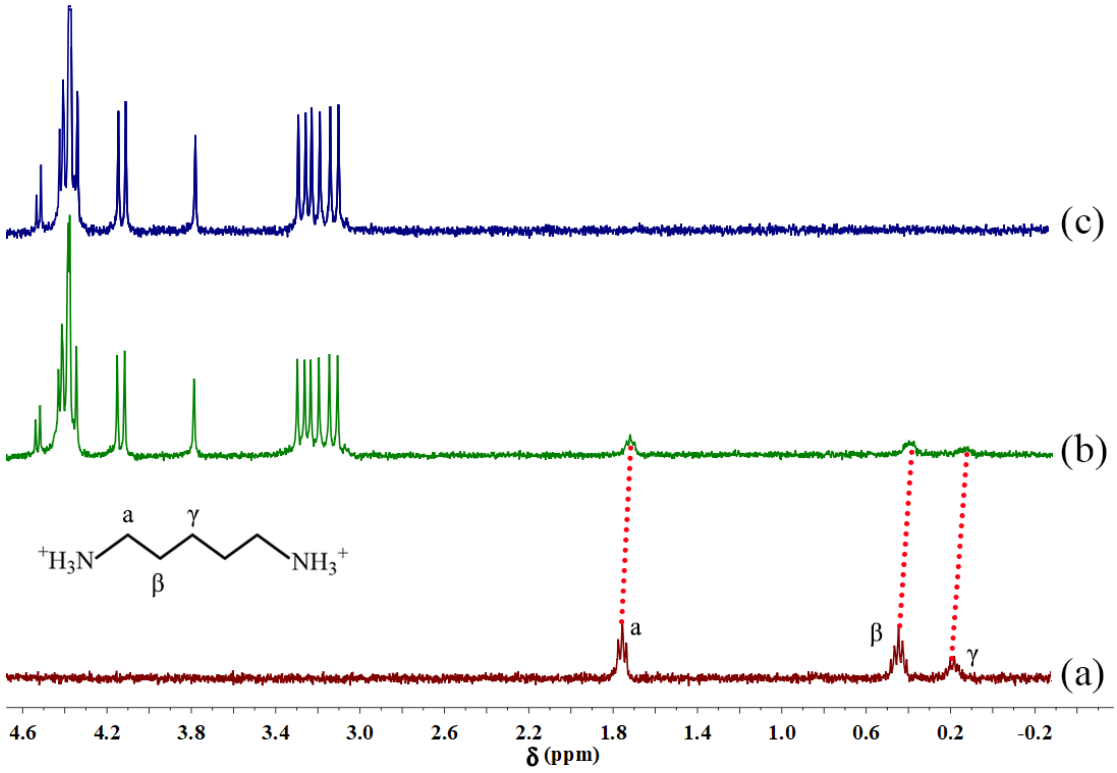

Figure 5. ^{1}H NMR spectra (400 MHz, 0.5 mL 4 mol/L DCl/D_2O); (a) ^{1}H NMR spectrum of guest 1,5-pentanediamine; (b) ^{1}H NMR spectrum of *i*Q[6] and guest 1,5-pentanediamine; (c) ^{1}H NMR spectrum of *i*Q[6].

4. Conclusion

In summary, we report the formation of a 1:1 supramolecular assemblies formed from 1,5-pentanediamine and *i*Q[6] molecules in HCl medium at 6 M, using $[ZnCl_4]^{2-}$ ions as a structural inducer. Single crystal X-ray diffraction analysis reveals that the $[ZnCl_4]^{2-}$ ions exhibit a typical "honeycomb effect" and are arranged in a honeycomb

structure repeating in a hexagonal pattern. The *i*Q[6] has various non-covalent interactions with the 1,5-pentanediamine guest, including hydrogen bonding interactions and ion-dipole interactions. The *i*Q[6] host forms a molecular chain through external surface interactions, which in turn fills in the hexagonal honeycomb structure formed by the $[ZnCl_4]^{2-}$ ion. ^{1}H NMR spectroscopy reveals that the alkyl chain part of the guest 1,5-pentanediamine is located in the cavity of the *i*Q[6] whilst the rest of it resides at the entrance of the cavity.

Acknowledgements

We acknowledge the support of Guizhou Provincial Science and Technology Projects (ZK[2023]General 040 and ZK[2022]General 552), TJP and CR thank the University of Hull for support.

References

[1] L. Yang, J. Kan, X. Wang, Y. Zhang, Z. Tao, Q. Liu, F. Wang, X. Xiao, Front. Chem., 6 (2018) 289.

[2] M. Papageorgiou, D. Lambropoulou, C. Morrison, E. Kłodzińska, J. Namieśnik, J. Płotka-Wasylka, TrAC Trends Anal. Chem., 98 (2018) 128-142.

[3] A. Jain, K.K. Verma, TrAC Trends Anal. Chem., 109 (2018) 62-82.

[4] P.H. Shan, Z.R. Zhang, D. Bai, B. Bian, Z. Tao, X. Xiao, New J. Chem., 43 (2019) 407-412.

[5] R. Michalski, P. Pecyna-Utylska, J. Kernert, J. Chromatogr. A, 1651 (2021) 462319.

[6] D. Gomes Müller, E. Quadro Oreste, M. Grazielle Heinemann, D. Dias, F. Kessler, Eur. Polym. J., 175 (2022) 111221.

[7] H. Vasconcelos, J.M.M.M. de Almeida, A. Matias, C. Saraiva, P.A.S. Jorge, L.C.C. Coelho, Trends Food Sci. Technol., 113 (2021) 86-96.

[8] L. Simon Sarkadi, Pure Appl. Chem., 91 (2019) 289-300.

[9] H. Zhu, S. Yang, Y. Zhang, G. Fang, S. Wang, Anal. Methods, 8 (2016) 3747-3755.

[10] M.A. Munir, K.H. Badri, J. Anal. Methods Chem., 2020 (2020) 5814389.

[11] D. Doeun, M. Davaatseren, M.S. Chung, Food Sci. Biotechnol., 26 (2017) 1463-1474.

[12] G. Zhang, A.S. Loch, J.C.M. Kistemaker, P.L. Burn, P.E. Shaw, J. Mat. Chem. C, 8 (2020) 13723-13732.

[13] K. Miller, C.L. Reichert, M. Schmid, Food Rev. Int., (2021) 1-25.

[14] M.A. Sahudin, M.S. Su'ait, L.L. Tan, Y.H. Lee, N.H. Abd Karim, Anal. Bioanal. Chem., 411 (2019) 6449-6461.

[15] J.J. Learey, S. Crawford-Clark, B.J. Bowen, C.J. Barrow, J.L. Adcock, J. Sep. Sci., 41 (2018) 4430-4436.

[16] P.B. Tsafack, A. Tsopmo, Heliyon, 8 (2022) e10456.

[17] F. Gardini, Y. Ozogul, G. Suzzi, G. Tabanelli, F. Ozogul, Front. Microbiol., 7 (2016) 1218.

[18] B. Li, S. Lu, Process Biochemistry, 99 (2020) 331-339.

[19] J.M. Lorenzo, P.E.S. Munekata, R. Domínguez, Curr. Opin. Food Sci., 14 (2017) 61-65.

[20] R. Torre, E. Costa-Rama, H.P.A. Nouws, C. Delerue-Matos, Biosensors (Basel), 10 (2020) 139.

[21] G. Munzi, S. Failla, S. Di Bella, Analyst, 146 (2021) 2144-2151.

[22] A.L. Jancewicz, N.M. Gibbs, P.H. Masson, Front. Plant Sci., 7 (2016) 870.

[23] W. Ma, K. Chen, Y. Li, N. Hao, X. Wang, P. Ouyang, Engineering, 3 (2017) 308-317.

[24] J. Becker, C. Wittmann, Curr. Opin. Biotechnol., 23 (2012) 631-640.

[25] G. Alvarez, L. Montero, L. Llorens, M. Castro-Puyana, A. Cifuentes, Electrophoresis, 39 (2018) 136-159.

[26] J. Sekula, J. Everaert, H. Bohets, B. Vissers, M. Pietraszkiewicz, O. Pietraszkiewicz, F. Du Prez, K. Vanhoutte, P. Prus, L.J. Nagels, Anal. Chem., 78 (2006) 3772-3779.

[27] A. Zotou, M. Notou, Anal. Bioanal. Chem., 403 (2012) 1039-1048.

[28] J. Lange, C. Wittmann, Anal. Bioanal. Chem., 372 (2002) 276-283.

[29] E. Kovács, J. Deme, G. Turczel, T. Nagy, V. Farkas, L. Trif, S. Kéki, P. Huszthy, R. Tuba, Polym. Chem., 10 (2019) 5626-5634.

[30] G. Yu, R. Zhao, D. Wu, F. Zhang, L. Shao, J. Zhou, J. Yang, G. Tang, X. Chen, F. Huang, Polym. Chem., 7 (2016) 6178-6188.

[31] G. Gattuso, A. Notti, M.F. Parisi, I. Pisagatti, P.M. Marcos, J.R. Ascenso, G. Brancatelli, S. Geremia, New J. Chem., 39 (2015) 817-821.

[32] J. Zhou, G. Yu, F. Huang, Chem. Soc. Rev., 46 (2017) 7021-7053.

[33] R. Behrend, E. Meyer, F. Rusche, Justus Liebig's Annalen der Chemie, 339 (1905) 1-37.

[34] J. Hu, Y. Huang, C. Redshaw, Z. Tao, X. Xiao, Coord. Chem. Rev., 489, (2023) 215194.

[35] D. Yang, X.n. Yang, M. Liu, L.x. Chen, Q. Li, H. Cong, Z. Tao, X. Xiao, Microporous Mesoporous Mater., 341 (2022) 112023.

[36] M. Liu, R. Cen, J. Li, Q. Li, Z. Tao, X. Xiao, L. Isaacs, Angew. Chem. Int. Ed. Engl, 61 (2022) e202207209.

[37] F.-F. Shen, J.-L. Zhao, K. Chen, Z.-Y. Hua, M.-D. Chen, Y.-Q. Zhang, Q.-J. Zhu, Z. Tao, CrystEngComm, 19 (2017) 2464-2474.

[38] Y. Huang, R.H. Gao, M. Liu, L.X. Chen, X.L. Ni, X. Xiao, H. Cong, Q.J. Zhu, K. Chen, Z. Tao, Angew. Chem. Int. Ed. Engl., 60 (2021) 15166-15191.

[39] X.L. Ni, X. Xiao, H. Cong, Q.J. Zhu, S.F. Xue, Z. Tao, Acc. Chem. Res., 47 (2014) 1386-1395.

[40] W. Zhang, Y. Luo, M.-H. Jia, X.-L. Ni, Z. Tao, C.-D. Xiao, X. Xiao, Sens. Actuators B Chem., 366 (2022) 132006.

[41] C. Gao, Q. Wang, J. Li, C.H.T. Kwong, J. Wei, B. Xie, S. Lu, S.M.Y. Lee, R. Wang, Sci. Adv., 8 (2022) eabn1805.

[42] C. Sun, Z. Wang, L. Yue, Q. Huang, Q. Cheng, R. Wang, J. Am. Chem. Soc., 142 (2020) 16523-16527.

[43] W. Zhang, Y. Luo, Y. Zhou, M. Liu, W. Xu, B. Bian, Z. Tao, X. Xiao, Dyes and Pigments, 176 (2020) 108235.

[44] R. Cen, M. Liu, J. Lu, W. Zhang, J. Dai, X. Zeng, Z. Tao, X. Xiao, Chin. Chem. Lett., 33 (2022) 2469-2472.

[45] W. Zhang, Y. Luo, X.-L. Ni, Z. Tao, X. Xiao, Chem. Eng. J., 446 (2022) 136954.

[46] T.T. Zhang, X.N. Yang, J.H. Hu, Y. Luo, H.J. Liu, Z. Tao, X. Xiao, C. Redshaw, Chem. Eng. J., 452 (2023) 138960.

[47] Z. Wang, C. Sun, K. Yang, X. Chen, R. Wang, Angew. Chem. Int. Ed. Engl., 61 (2022) e202206763.

[48] L. Isaacs, S.K. Park, S. Liu, Y.H. Ko, N. Selvapalam, Y. Kim, H. Kim, P.Y. Zavalij, G.H. Kim, H.S. Lee, K. Kim, J. Am. Chem. Soc., 127 (2005) 18000-18001.

[49] R.V. Pinjari, S.P. Gejji, J. Phys. Chem. A, 113 (2009) 1368-1376.

[50] H.-Y. Wang, Y. Zhou, J.-H. Lu, Q.-Y. Liu, G.-Y. Chen, Z. Tao, X. Xiao, Arab. J. Chem., 13 (2020) 2271-2275.

[51] L.-L. Liang, Y. Zhao, K. Chen, X. Xiao, J. Clegg, Y.-Q. Zhang, Z. Tao, S.-F. Xue,

Q.-J. Zhu, G. Wei, Polymers, 5 (2013) 418-430.

[52] K. Chen, J. Xu, S.-C. Qiu, Y. Wang, M.-D. Chen, Y.-Q. Zhang, X. Xiao, Z. Tao, J. Mol. Struct., 1146 (2017) 402-408.

[53] S.-C. Qiu, Q. Li, J. Zhang, Z.-Z. Gao, Y.-Q. Zhang, S.-F. Xue, Q.-J. Zhu, X. Xiao, Z. Tao, J. Incl. Phenom., 86 (2016) 1-5.